S1: Measurement setup

To sample air Campbell Scientific AP200 intake assembly used. It has a filter that removes particulates, and a rain diverter to admit a sample of ambient air without allowing precipitation to enter. The intake assembly includes a mixing volume to dampen fluctuations in water vapor com concentrations. To prevent condensation, the water vapor sampling lines were equipped with heating cables running along their length. At 1.5m an automated weather station (AcuRite Iris 06014 PRO) was installed which measures temperature, relative humidity, wind speed and atmospheric pressure. For temperature and relative humidity at the four inlets, a HOBO External Temperature/RH Sensor Data Logger (Model MX2302A) is used. These sensors have a range of -40 to 70°C, resolution 0.02°C, and accuracy of ±0.25°C from -40 to 0°C and ±0.2°C. For RH, the measurement range is 0-100%, resolution 0.01%, accuracy from 0 to 70°C ±2.5% from 10% to 90% to a maximum of ±3.5%; below 10% RH and above 90% RH ±5%. For soil moisture and soil temperature measurements, HOBO MX Soil Moisture and Temperature Data Logger is used. This sensor has a measurement range of 0.00 to 0.64 m^3/m^3 and an accuracy of ±0.031 m^3/m^3 and resolution 0.001 m^3/m^3 for soil moisture. For soil temperature, resolution of the sensor is 0.04°C and the accuracy is ±0.25°C from -40 to 0°C ±0.45, ±0.2°C from 0 to 70°C.

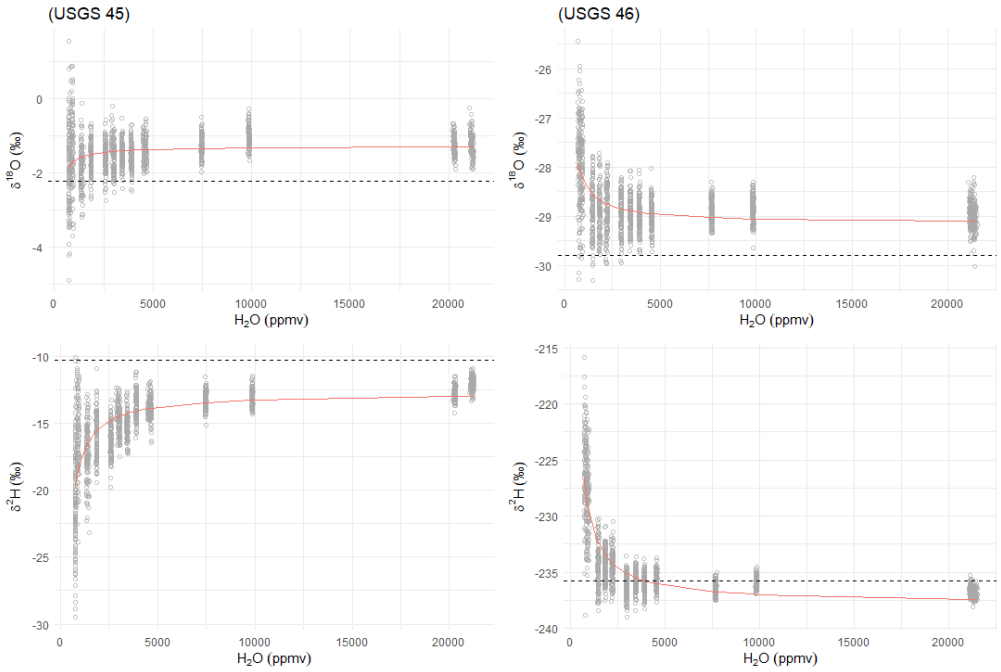

Figure S1 Humidity response calibrations for $\delta^{18}O$ and $\delta^{2}H$ of USGS standards 45 and 46. Grey circles represent individual 1s measurements, and the solid line shows the non-linear regression used to correct ambient isotope data as a function of cavity humidity. Dashed line shows the known isotopic value of the standard water.

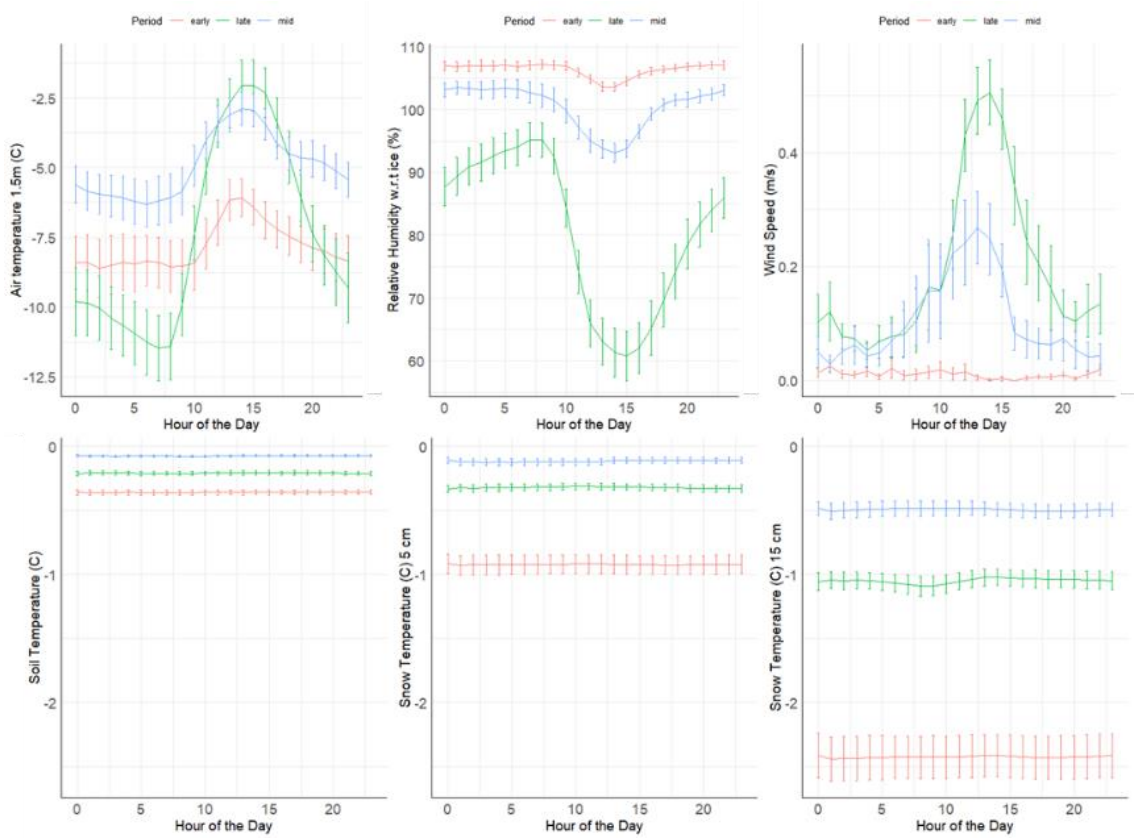

Figure S2 Plots depicting diurnal patterns in ambient air temperature (C), relative humidity w.r.t. ice (%), wind speed (m/s), and soil and snow temperatures (5cm and 15cm) depth, measured over three distinct periods: early, mid, and late.

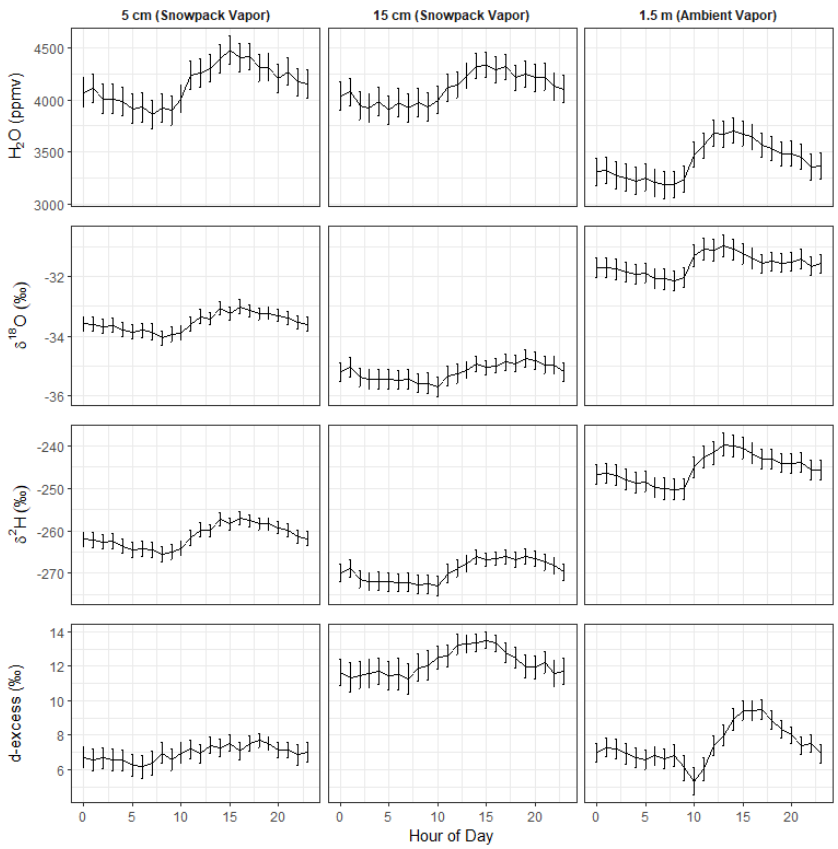

Figure S3 Diurnal variation in water vapor mixing ratio (H_2O, top row), $\delta^{18}O$ (second row), δ^2H (third row), and d-excess (bottom row) at three sampling heights in and above the snowpack: 5 cm (Snowpack Vapor), 15 cm (Snowpack Vapor), and 1.5 m (Ambient Vapor). Symbols show mean values by hour; error bars represent the standard error.

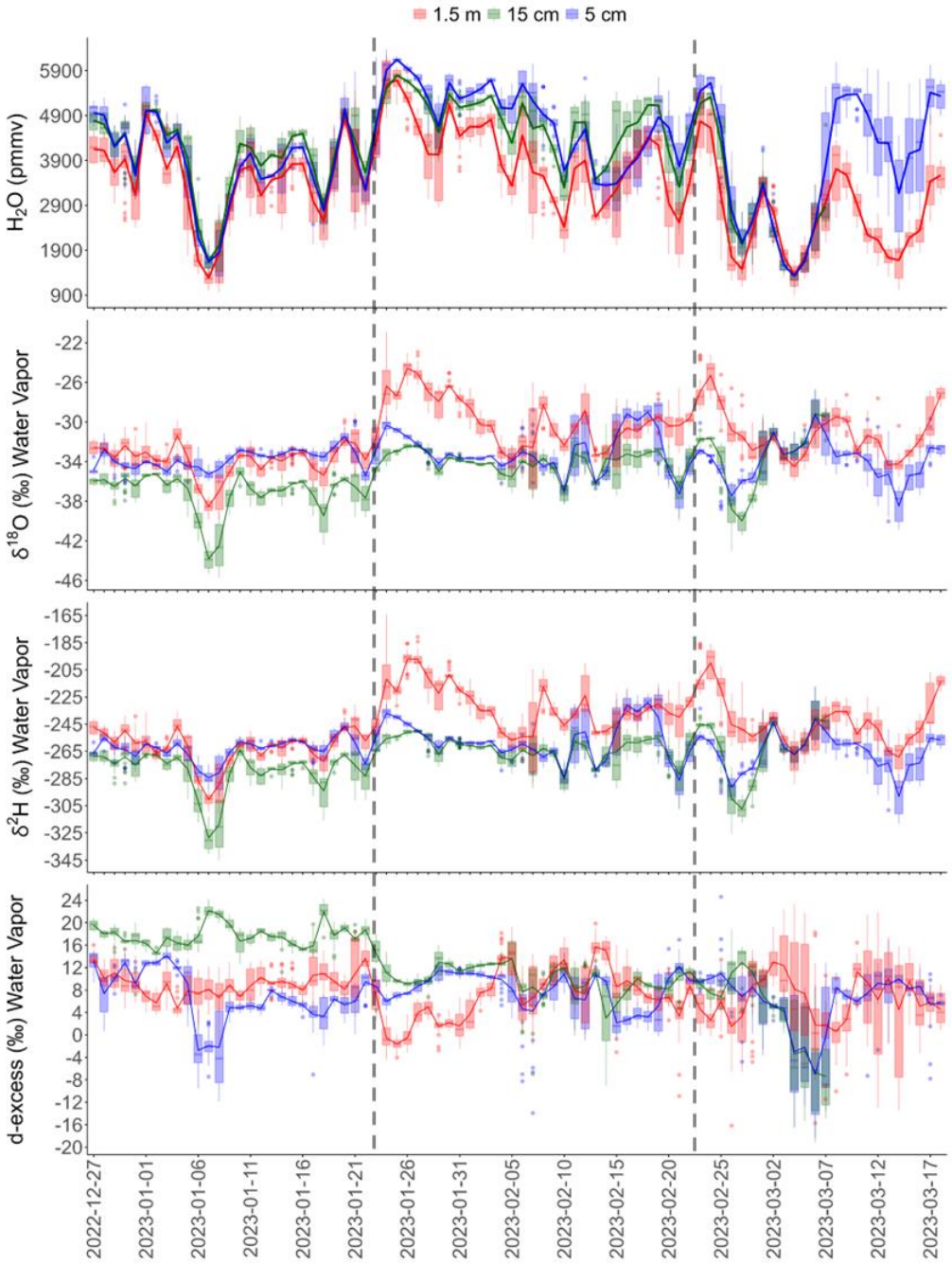

Figure S4 water vapor concentration, and isotopic composition $\delta^{18}O$, $\delta^{2}H$, and d-excess at 5 cm (blue), 15 cm (green) and 1.5m (red). The bars represent the diurnal variability, and the lines join the daily mean values. The dataset is classified into three distinct periods—early, mid, and late - the vertical dotted lines represent key transitions between these periods: January 24, 2023, marks the onset of the first significant warm event, ending the early period, which serves as a baseline for pre-event climatic conditions. February 23, 2023, marks the beginning of the second warm event, transitioning from the mid period to the late period. The late period includes observations post the second warm event.

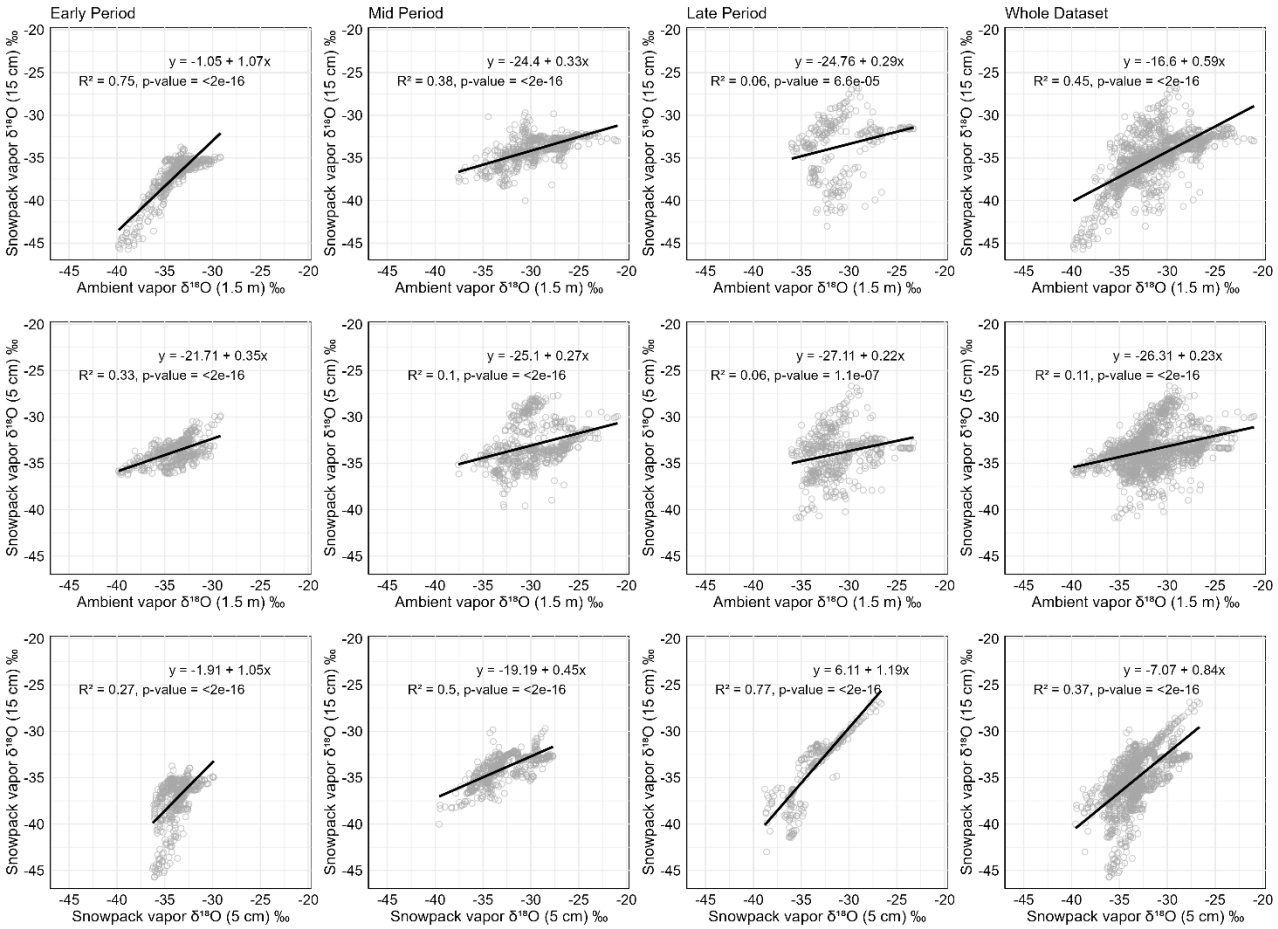

Figure S5 Correlation plots displaying the relationship between ambient vapor $\delta^{18}O$ at 1.5 m and snowpack vapor $\delta^{18}O$ at 5 cm across different seasonal periods and the entire dataset. Each plot illustrates linear regressions with respective slopes, R^2 values, and p-values.

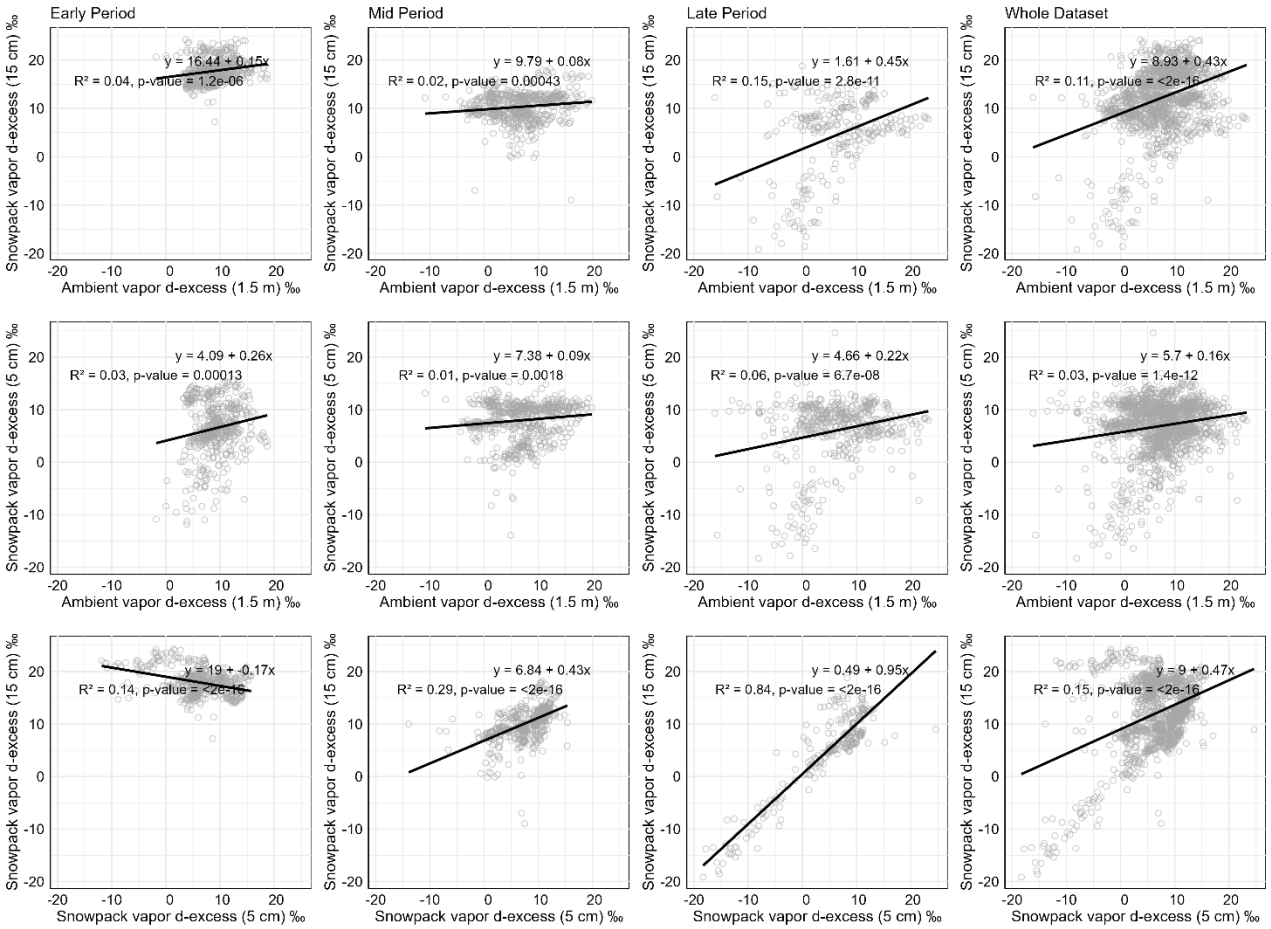

Figure S6 Scatter plots showing the correlation between ambient vapor d-excess at 1.5 m and snowpack vapor d-excess at 5 cm across different seasonal periods (Early, Mid, Late) and the entire dataset. Each plot includes linear regression lines with corresponding slopes, R^2 values, and p-values.

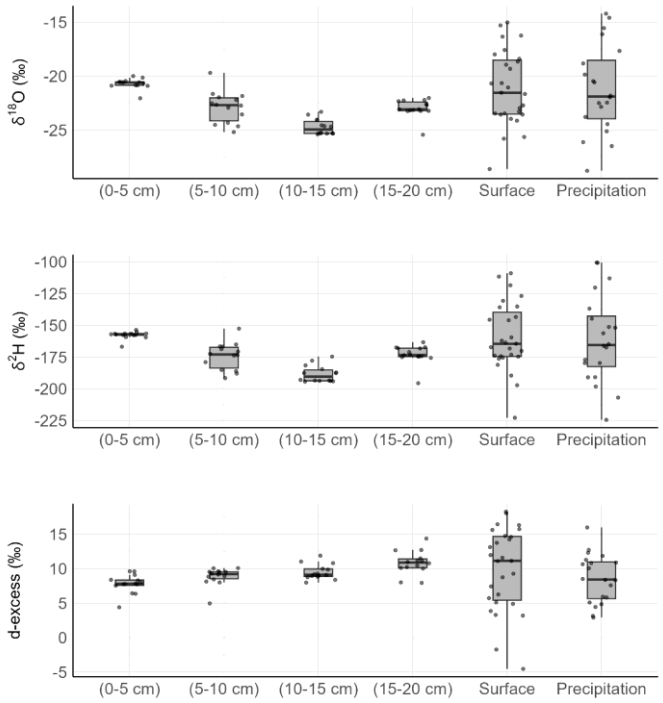

Figure S7 Boxplots of $\delta^{18}O$ (top panel), $\delta^{2}H$ (middle panel), and d-excess (bottom panel) across snow layers (0–5 cm, 5–10 cm, 10–15 cm, and 15–20 cm from ground level), Surface snow, and Precipitation. The boxes represent the interquartile range, the central line represents the median, whiskers indicate variability outside the upper and lower quartiles, and individual points denote outliers.

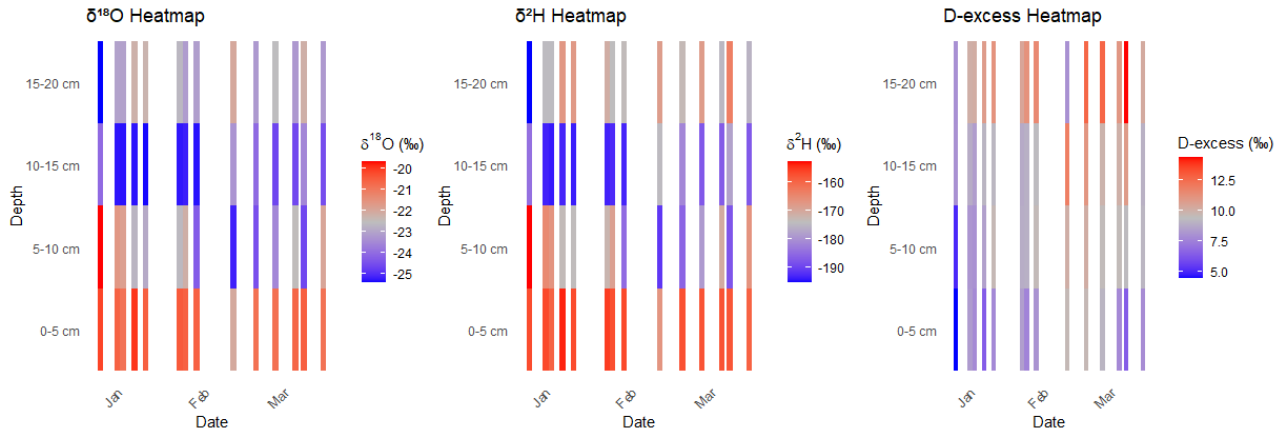

Figure S8 Heatmaps showing the depth and temporal variations in the isotopic composition of the snowpack for (a) $\delta^{18}O$, (b) $\delta^{2}H$, and (c) d-excess. Depths range from 0–5 cm to 15–20 cm.

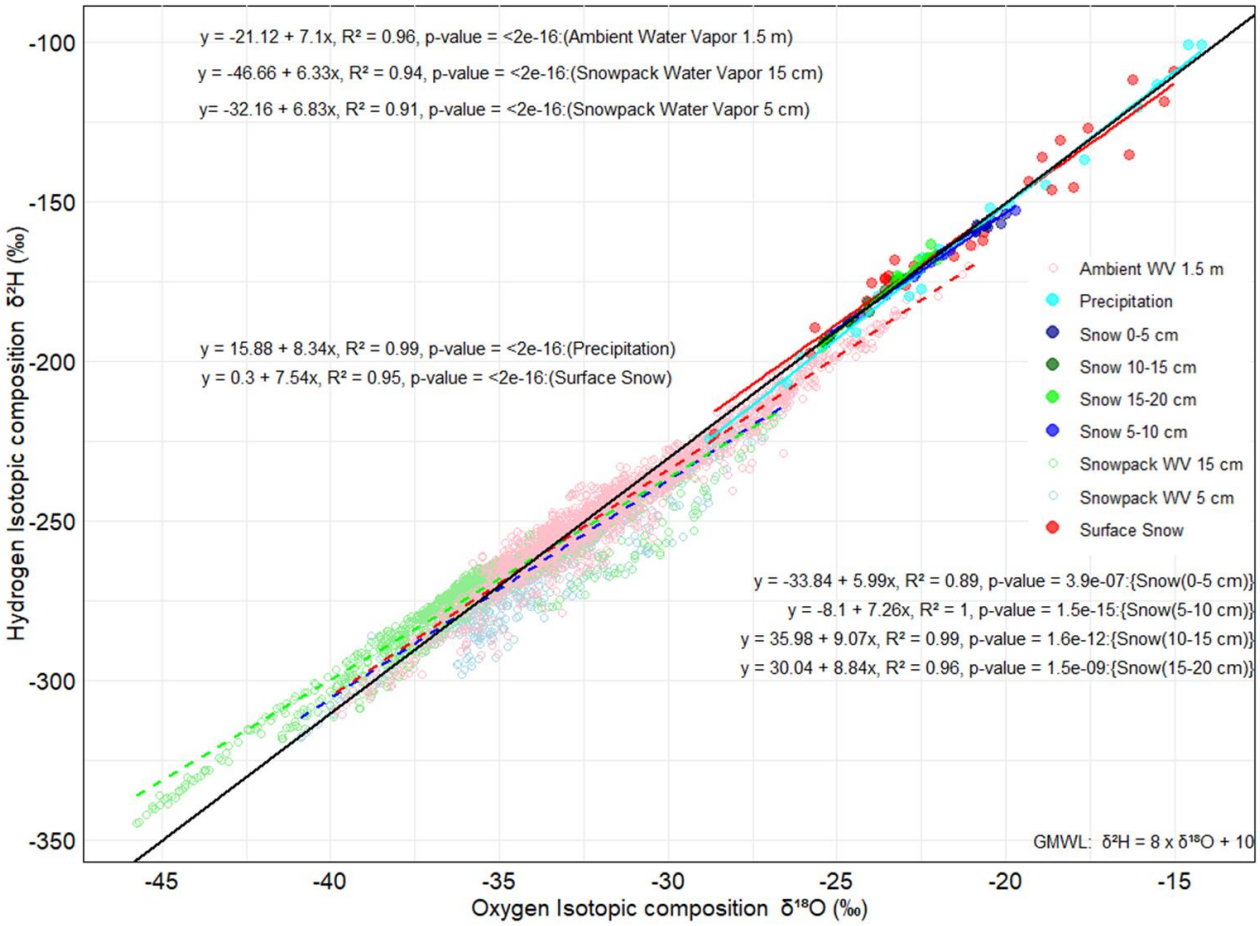

Figure S9 the relationships between hydrogen and oxygen isotopic compositions (δ^2H and $\delta^{18}O$) for different samples. Each color-coded data point represents a different sample type as indicated in the legend. The linear regression lines for each sample type display their respective isotopic relationships, annotated with their equations, R^2 values, and p-values. The Global Meteoric Water Line (GMWL) (solid black line) is also plotted for reference

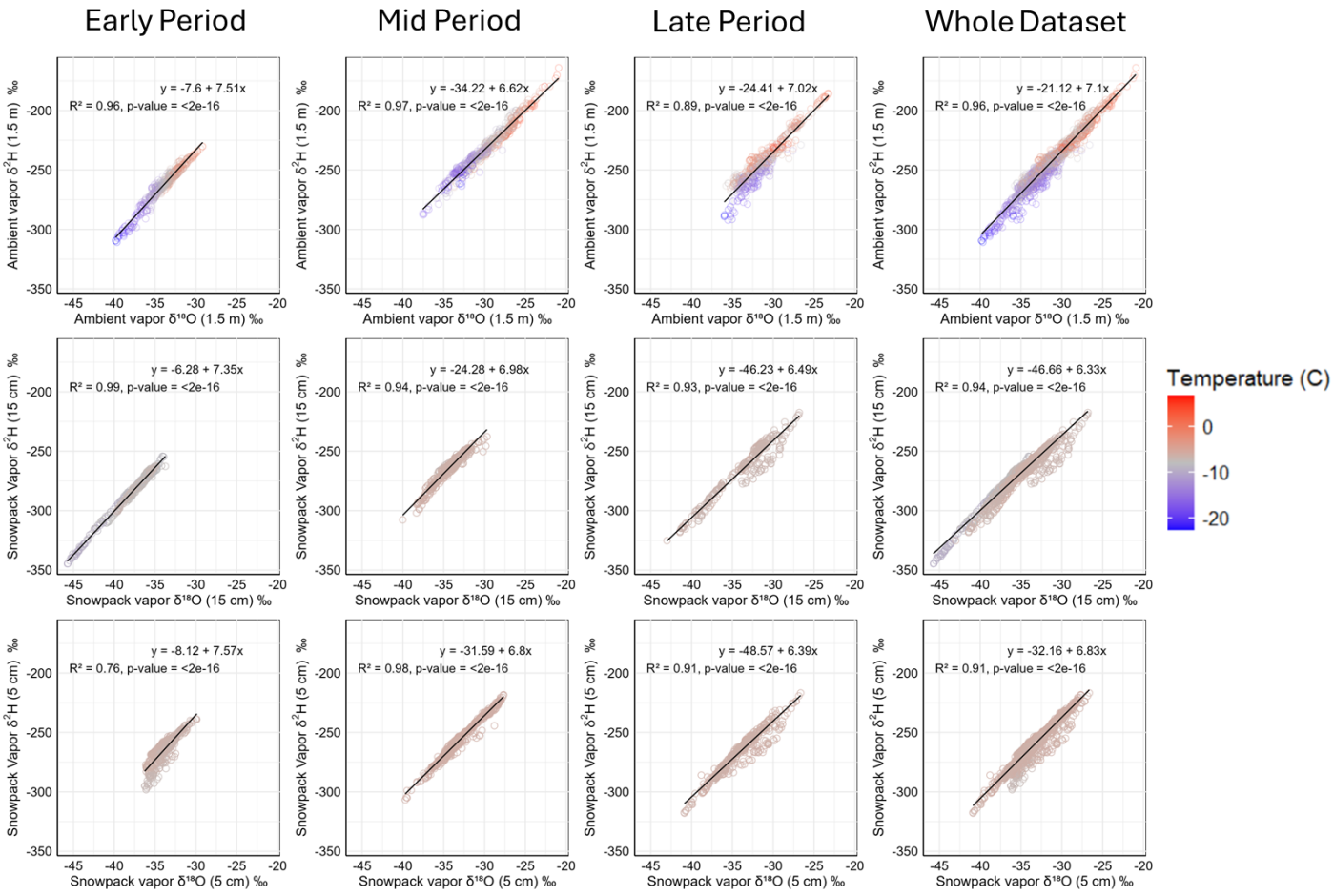

Figure S10 the relationships between $\delta^{18}O$ and $\delta^{2}H$ isotopic compositions in snowpack vapor at two distinct depths: 15 cm and 5 cm, alongside ambient measurements at 1.5 meters, measured across different periods: Early, Mid, Late, and the entire dataset (Whole). Each plot is color-coded to represent temperature variations at the corresponding measurement point. Linear regression lines are fitted to each dataset, with their equations, R^2 values, and p-values displayed.

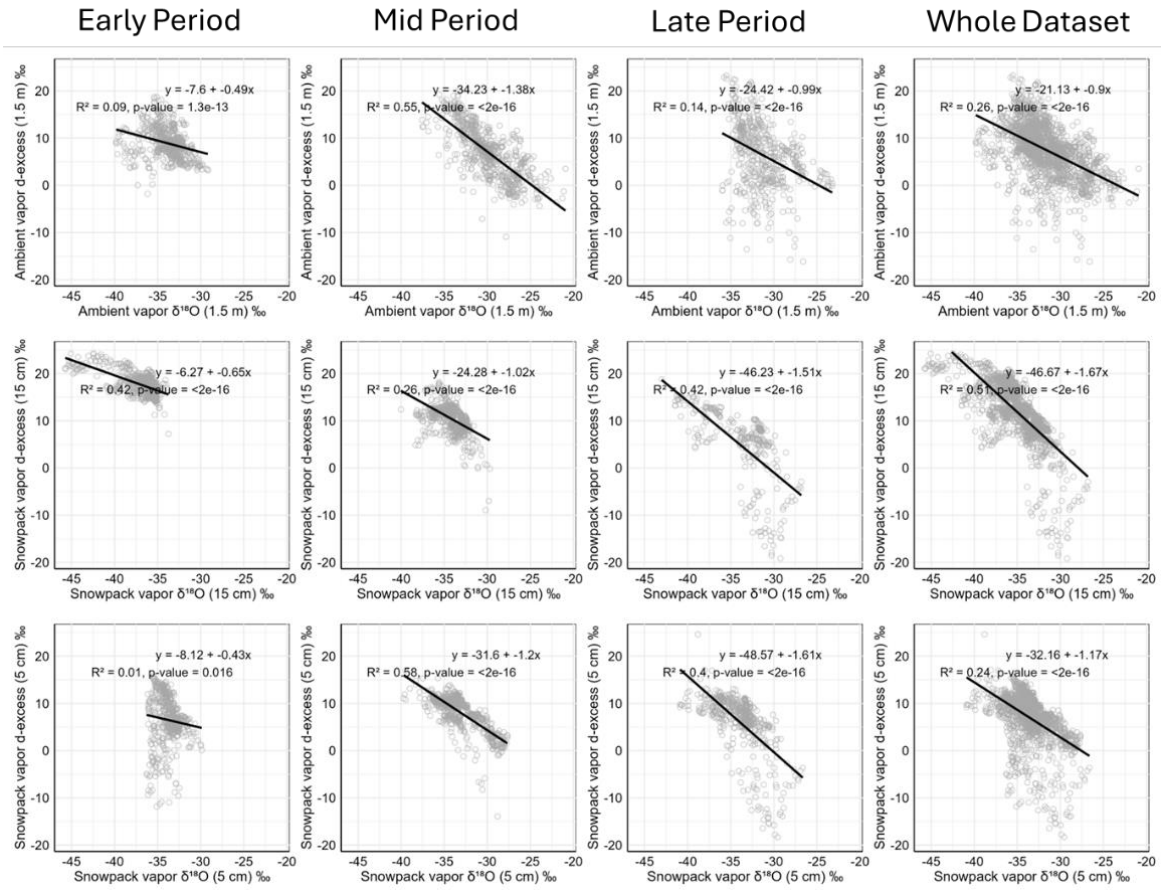

Figure S11 Relationships between δ¹⁸O and d-excess for ambient vapor at 1.5 m (top row), snowpack vapor at 15 cm (middle row), and snowpack vapor at 5 cm (bottom row) during the early, mid, late periods, and for the entire dataset. Each panel displays the regression equation, coefficient of determination (R^2), and p-value.

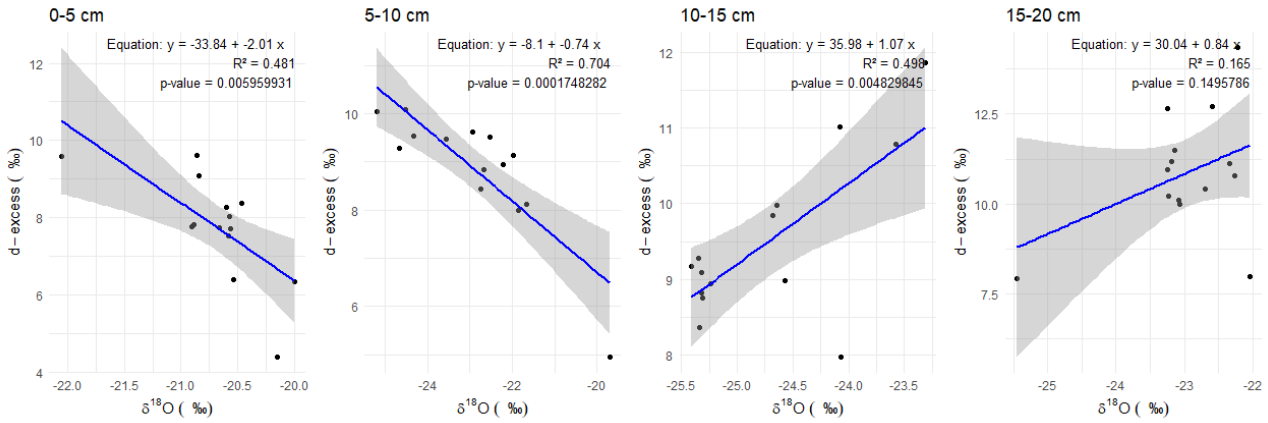

Figure S12 The series of plots illustrate the linear regression analysis of δ¹⁸O and d-excess values across different snow layers at depths of 0-5 cm, 5-10 cm, 10-15 cm, and 15-20 cm. Each plot displays a regression line (blue) with the corresponding shaded area representing the confidence interval.

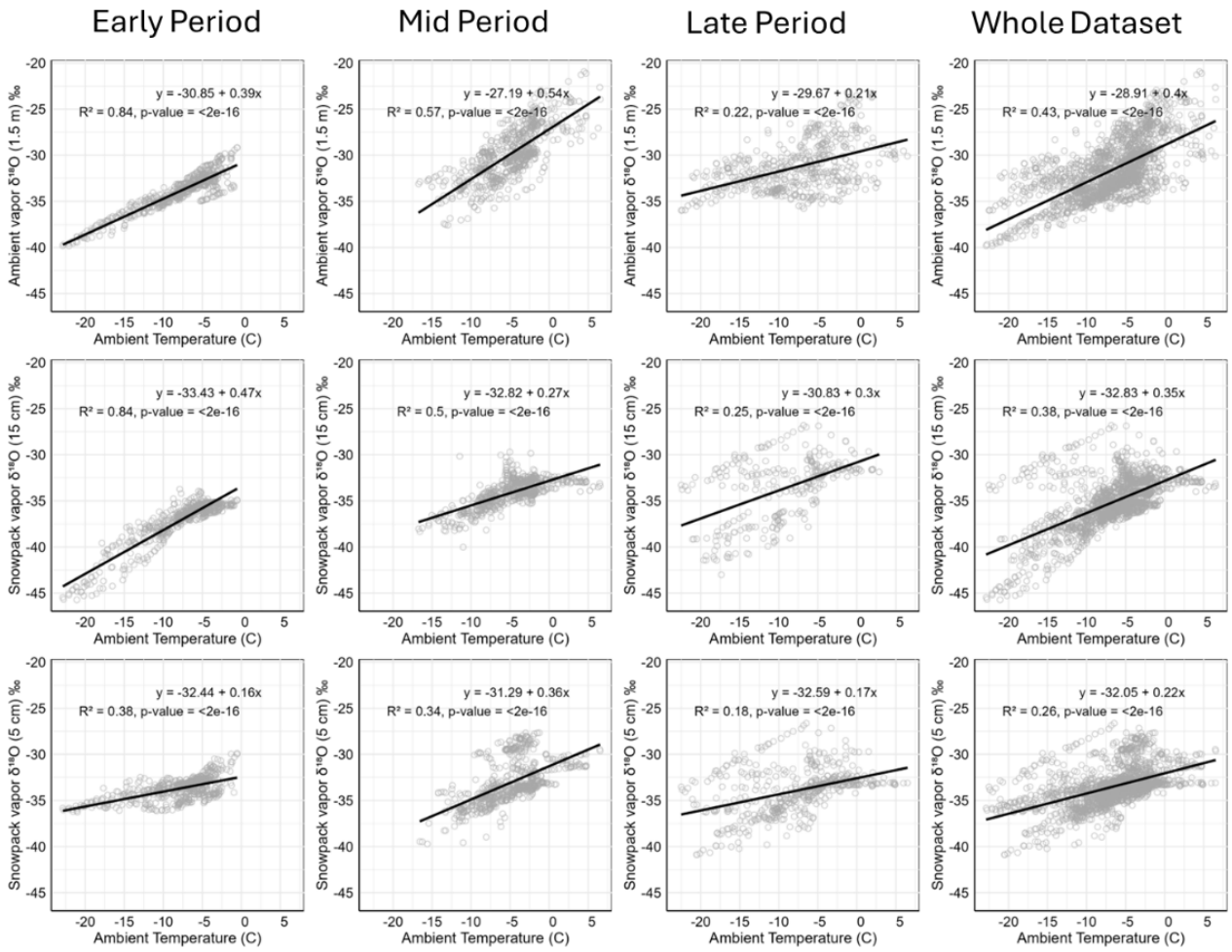

Figure S13 The plots illustrate the relationship between ambient temperature and the isotopic composition of water vapor ($\delta^{18}O$) at different heights (1.5 m, 15 cm, 5 cm) across periods (Early, Mid, Late) and for the entire dataset.

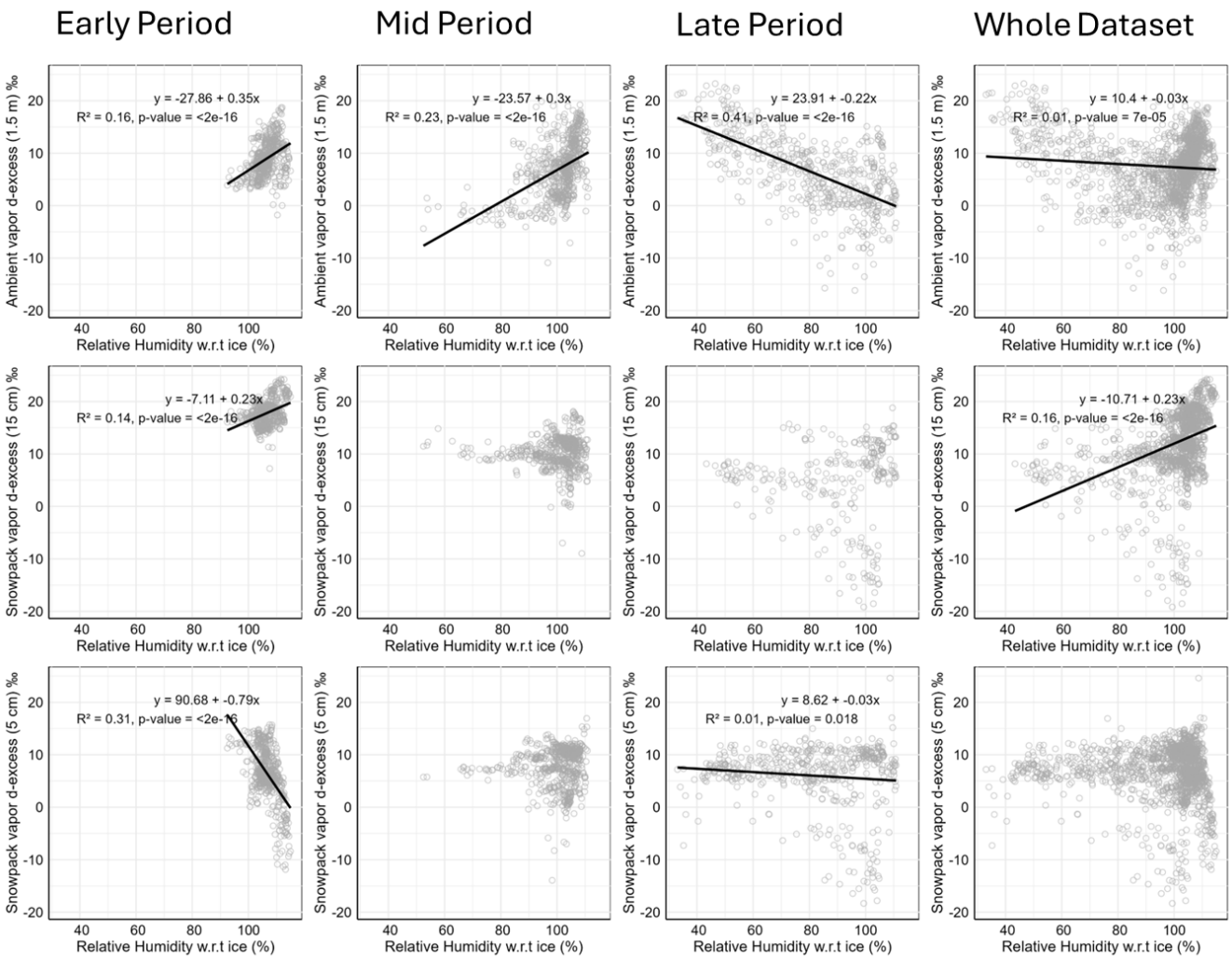

Figure S14. Relationships between relative humidity (Rel. Hum. Ice Ambient %) and vapor d-excess across different periods (Early, Mid, Late) and for the entire dataset. Each panel shows regression lines and statistical metrics (R^2 values and p-values) for ambient vapor and vapor at two different heights in the snowpack (5 m and 15 m).

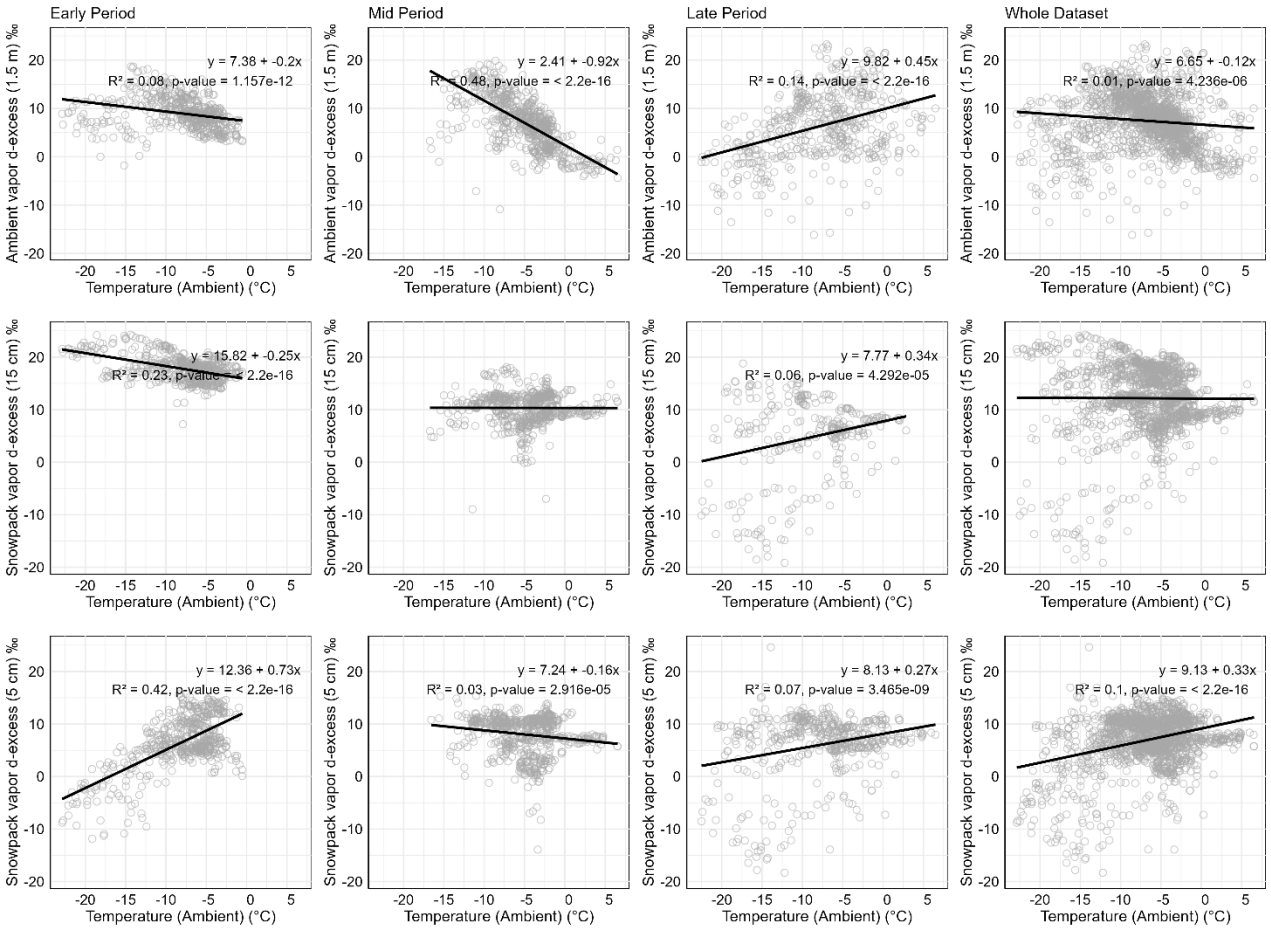

Figure S15 Relationship between ambient air temperature and vapor d-excess across different periods (Early, Mid, Late) and for the entire dataset. Each panel shows regression lines and statistical metrics (R^2 values and p-values) for ambient vapor and vapor at two different heights in the snowpack (5 m and 15 m).

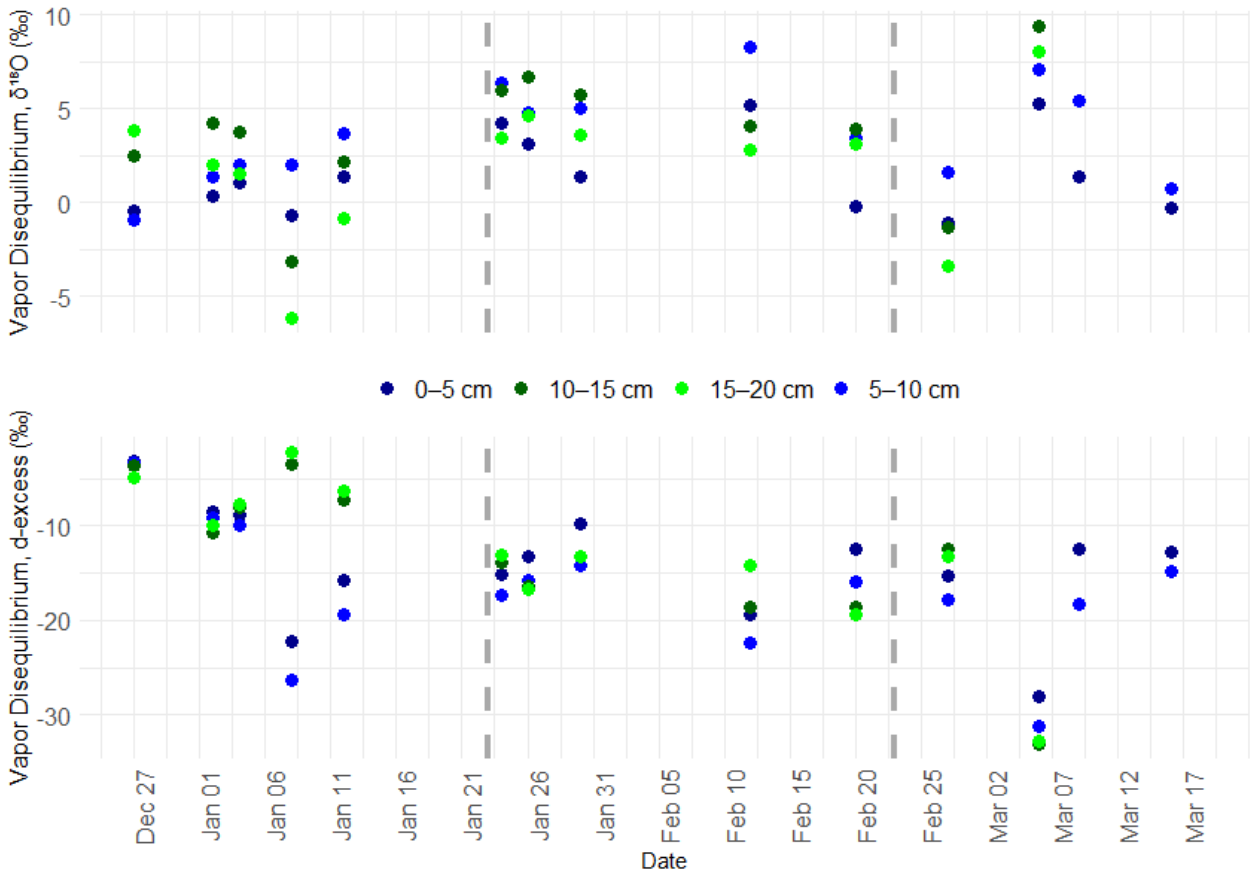

Figure S16 Temporal variations in vapor disequilibrium, shown as (a) $\delta^{18}O$ disequilibrium and (b) d-excess disequilibrium, measured at four depths (0–5 cm: dark blue; 5–10 cm: light blue; 10–15 cm: dark green; 15–20 cm: light green). Vertical dashed lines demarcate early, mid and late periods.

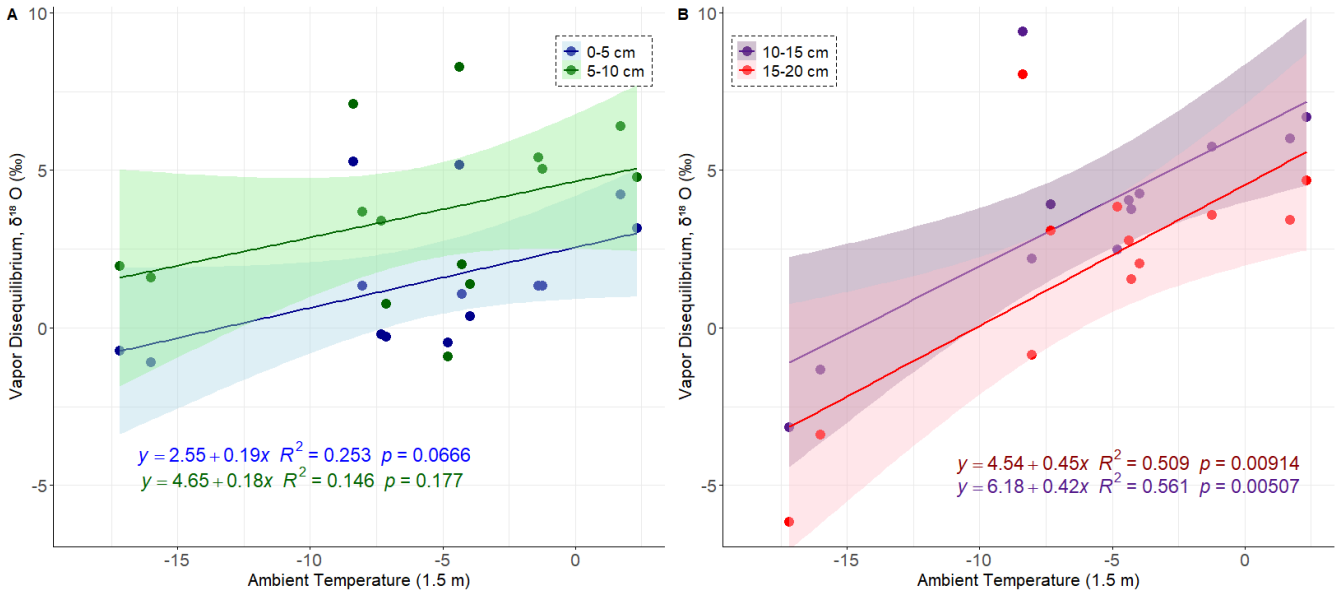

Figure S17 Scatter plots depicting the relationship between ambient temperature and disequilibrium (the difference in isotopic composition between measured and equilibrium vapor isotopic composition) and at various snowpack depths. The differences are calculated for two depth intervals: 0-5 cm and 5-10 cm in the left plot, and 10-15 cm and 15-20 cm in the right plot.

Table 1 presents the statistical summary of water vapor concentration (H_2O), $\delta^{18}O$, $\delta^{2}H$, and d-excess(d-ex) at three measurement heights: Snowpack 5 cm, Snowpack 15 cm, and Ambient 1.5 m. The data is categorized into three periods: Early, Mid, and Late, along with overall statistics for all periods combined. For each variable, the table displays the number of observations (n), minimum and maximum values, and mean ± standard deviation. The dataset is classified into three distinct periods, early, mid, and late - the vertical dotted lines represent key transitions between these periods: January 24, 2023, marks the onset of the first significant warm event, ending the early period, which serves as a baseline for pre-event climatic conditions. February 23, 2023, marks the beginning of the second warm event, transitioning from the mid period to the late period. The late period includes observations post the second warm event.

d-ex mean±sd	d-ex max	d-ex min	$\delta^{2}H$ mean±sd	$\delta^{2}H$ max	$\delta^{2}H$ min	$\delta^{18}O$ mean±sd	$\delta^{18}O$ max	$\delta^{18}O$ min	H_2O mean±sd	H_2O max	H_2O min	n		Period
6.93 ± 5.03	24.62	-18.32	-261.36 ± 15.02	-216.74	-317.84	-33.54 ± 2.1	-26.64	-40.89	4150.28 ± 1246.4	6363.81	1088.22	1755	Snowpack 5 cm	Overall
6.48 ± 5.06	15.72	-11.85	-263.44 ± 10.24	-238.69	-298.18	-33.74 ± 1.18	-29.88	-36.27	3730.38 ± 1003.84	5879.48	1155.8	567		Early
8 ± 3.64	16.95	-13.92	-256.48 ± 15.97	-218.2	-306.65	-33.06 ± 2.32	-27.67	-39.71	4791.8 ± 888.45	6363.81	2395.46	677		Mid
6.03 ± 6.21	24.62	-18.32	-265.54 ± 16.37	-216.74	-317.84	-33.95 ± 2.45	-26.64	-40.89	3766.29 ± 1512.68	6085.89	1088.22	511		Late
12.17± 6.45	24.29	-19.16	-269.49 ± 18.09	-217.45	-344.7	-35.21 ± 2.77	-26.81	-45.73	4104.36 ± 1181.83	5872.75	1077.35	1532	Snowpack 15 cm	Overall
17.76 ± 2.32	24.29	7.22	-279.42 ± 17.26	-254.15	-344.7	-37.15 ± 2.33	-33.74	-45.73	3953.89 ± 965.55	5258.02	1192.25	593		Early
10.34 ± 2.97	18.13	-8.96	-262.48 ± 10.75	-237.75	-307.74	-34.1 ± 1.49	-29.7	-40.02	4763.16 ± 749.17	5872.75	2241.36	661		Mid
4.59 ± 8.05	18.79	-19.16	-264.96 ± 23.4	-217.45	-325.28	-33.69 ± 3.48	-26.81	-43.01	2858.88 ± 1322.5	5635.98	1077.35	278		Late
7.43 ± 5.35	23.25	-16.16	-245.31 ± 21.97	-163.96	-310.76	-31.59 ± 3.03	-20.93	-39.82	3416.64 ± 1139.48	6249.24	895.34	1824	Ambient 1.5 m	Overall
8.93 ± 3.15	18.69	-1.79	-262.25 ± 14.67	-230.17	-310.76	-33.9 ± 1.91	-29.17	-39.82	3443.61 ± 1009.9	5460.45	963.4	600		Early
6.91 ± 5.22	19.86	-10.89	-231.76 ± 18.93	-163.96	-287.79	-29.83 ± 2.81	-20.93	-37.57	3993.52 ± 965.85	6249.24	1525.87	694		Mid
6.4 ± 6.91	23.25	-16.16	-243.86 ± 19.53	-185.4	-292.12	-31.28 ± 2.63	-23.22	-35.99	2630.74 ± 1020.44	5567.03	895.34	530		Late